Light polarizer in visible and THz range based on single-wall carbon nanotubes embedded into poly(methyl methacrylate) film

2016 Laser Phys. Lett. 13 065901

(http://iopscience.iop.org/1612-202X/13/6/065901)

IOP Publishing | Astro Ltd
Laser Physics Letters
Laser Phys. Lett. **13** (2016) 065901 (5pp)
doi:10.1088/1612-2011/13/6/065901

Light polarizer in visible and THz range based on single-wall carbon nanotubes embedded into poly(methyl methacrylate) film

N R Arutyunyan[1,2], M A Kanygin[3,4], A S Pozharov[1], V V Kubarev[5], L G Bulusheva[3,4], A V Okotrub[3,4] and E D Obraztsova[1,2]

[1] A.M. Prokhorov General Physics Institute, 38 Vavilov Str., 119991 Moscow, Russia
[2] National Research Nuclear University 'MEPhI', 31 Kashirskoe Sh., 115409 Moscow, Russia
[3] Nikolaev Institute of Inorganic Chemistry, 3 Acad. Lavrentiev Ave., 630090 Novosibirsk, Russia
[4] Tomsk State University, 36 Lenin Ave., 634050 Tomsk, Russia
[5] Budker Institute of Nuclear Physics, SB RAS, 11 Acad. Lavrentiev Ave., 630090 Novosibirsk, Russia

E-mail: natalia.arutyunyan@gmail.com

Received 30 March 2016
Accepted for publication 14 April 2016
Published 4 May 2016

Abstract

Poly(methyl metacrylate) samples with uniformly dispersed single-wall carbon nanotubes (SWCNTs) were mechanicaly stretched up to 4 times at 150 °C. As a result, SWCNTs were oriented preferentially along the stretch direction. The width of the angular distribution of the SWCNT orientation determined by polarized Raman scattering and THz absorption spectroscopy was 15 and 12°, respectively. Both methods revealed a high anisotropy of optical response of the composite film. Its application as an efficient polarizer in a wide spectral range from visible to THz is promising.

Keywords: carbon nanotubes, THz spectroscopy, Raman spectroscopy, anisotropy, polymer-matrix composites

(Some figures may appear in colour only in the online journal)

Terahertz (THz) radiation is widely used in different fields like astronomy, spectroscopy, telecommunications, medical and security screening, etc owing to unique properties inherent to low-energy photons. During the last two decades, efficient emitters, detectors, and other components for THz technologies were developed [1–7]. Among them, high performance polarizers as quasioptical devices for manipulation of THz waves are highly demanded. Several kinds of novel THz polarizers such as liquid crystal polarizers, Brewster's angle polarizers and wire-grid polarizers [8–14] have been developed basing on different technologies. The structures composed of uniformly spaced metal wires exhibited the high extinction coefficients at THz wavelengths, although they had drawbacks of fragility and structurally tuned architecture not extendable to the broadband THz operation [10].

Carbon nanotubes (CNTs) effectively interact with radiation in the whole frequency range form UV to THz. The isolated SWCNT may be regarded as a 1D object. A small diameter (about 1 nm) and a mean length (few hundreds nm) determine a high aspect ratio of nanotubes. As a consequence, the effects of anisotropic interaction of SWCNTs with the polarized radiation can be observed in processes of light absorption, scattering and so forth. It allows creating anisotropic materials with nanotubes aligned along the preferable direction [15–18], which is quite promising for fabrication of novel optical elements.

Various methods were proposed to form the structures of ordered CNTs. Recently, it was proposed to guide the growth of SWCNTs, using the Y-cut of single-crystal quartz substrates [19] and sapphire [20]. It should be mentioned, however, that

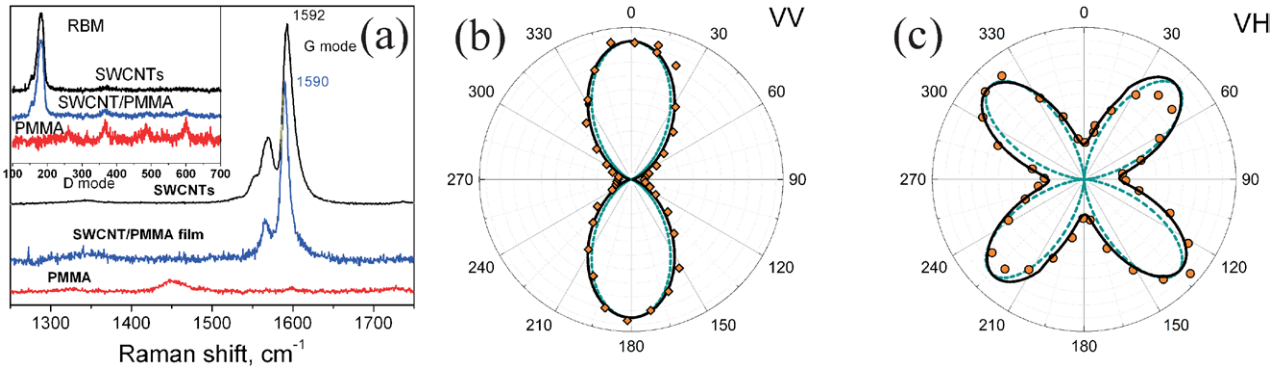

Figure 1. (a) Raman spectra of raw SWCNTs, stretched PMMA film with and without SWCNTs. The excitation laser wavelength is 514.5 nm. The inset demonstrates the low-frequency range and the RBM of SWCNTs. (b) and (c) The *G*-mode intensity of stretched SWCNT/PMMA film as a function of the sample orientation, measured in VV ((b), diamonds) and VH ((c), circles) configurations. The theoretical curves corresponding to $\cos^4(\theta)$ and $\sin^2(\theta)\cos^2(\theta)$ for VV and VH configurations are shown by dashed lines. The angular distribution of SWCNTs (solid lines) is 15°.

the density of nanotubes is strongly correlated with the density of step edges and, consequently, it is difficult to vary it in a wide spectral range, especially, when the uniform close-packed structures are needed.

The idea to use a self-assembly process of CNTs was realized with spin-assembly technique [21], mechanical shearing [22, 23], DNA-assisted liquid crystal formation on hydrophilic layers [24]. A very narrow angular distribution of the SWCNT orientation was demonstrated by means of Langmuir–Blodgett assembly [25] and self-alignment into micron-wide strips [26]. It has been shown that nanotubes tend to orient themselves in the suspension, aligning parallel to the 'triple line' liquid–air–substrate [27, 28].

Stretching of polymer matrix with embedded SWCNTs is a prospective method due to its easy reproduction. The strong anisotropy of optical absorption, fluorescence and Raman scattering has confirmed the preferable orientation of nanotubes along the stretch direction [29–33]. Though this method has a natural limit of nanotube alignment (a finite limit of polymer strain) and no complete alignment or suppression can be achieved, it demonstrated a very good reproducibility and provided an easy mass production.

In this paper, we oriented SWCNTs in poly (methyl metacrylate) (PMMA) matrix by uniaxial stretching of composite. The alignment of SWCNTs was estimated by polarized Raman and THz absorption spectroscopy. The composite film exhibited a high anisotropy of optical properties in a wide spectral range, from THz to visible.

SWCNTs were produced by arc-discharge method, the mean diameter was 1.35 nm [34, 35]. Raw nanotubes were dispersed in chloroform; the bundles of nanotubes were disagregated by the ultrasonic tip *Hielscher UP200* at the power of 200 W during 1 h. The dispersion of SWCNTs was added to PMMA (10 wt%) solution in chloroform and mixed at a magnetic stirrer during 2 h. The weight content of SWCNTs in the final suspension was 0.01%. The suspension was poured into a Petri cup, chloroform was evaporated during 24 h, and after that a free-standing composite film was formed. The film thickness was about 0.5 mm.

To align SWCNTs along a certain direction, the composite film was stretched uniaxially. PMMA is a thermoplastic polymer, which becomes stretchable at temperature above 120 °C. The film, placed between two clamps, was heated by a heat gun up to 150 °C. Then, one of the clamps moved with a constant speed 0.15 mm min^{-1}, and the film was stretched up to four times.

Raman scattering in SWCNTs was excited by radiation of Ar–Kr ion laser (*Spectra Physics)* with a wavelength of 514.5 nm. The scattered light was registered in the back-scattering geometry. The Raman spectra were recorded using a triple spectrometer Jobin Yvon S3000 with a resolution of 2 cm^{-1}. The film was placed on a rotating plate at the entrance of the spectrometer. The polarized Raman spectra were measured in parallel (VV) and crossed (VH) orientations of the polarization of the incident and scattered light.

The anisotropic electromagnetic response in the THz frequency range was measured by two independent ways: first, by the Fourier spectrometer and, second, with the Novosibirsk free electron laser (NFEL). The transmission spectra were recorded at normal incident angle of linear polarized beam with the parallel and perpendicular orientations of the electric field vector respectively to the stretching direction using a Bruker IFS 66vs vacuum Fourier spectrometer supplied with a pyroelectric detector for the range 30–700 cm^{-1}. The stretched SWCNT/PMMA film was exposed by 1 W linear polarized laser beam and rotated around the beam axis.

A typical resonant Raman spectrum of arc-discharge SWCNTs is shown in figure 1(a). In case when the laser excitation wavelength is 514.5 nm, the radial breathing modes (RBM) have a maximum at 180 cm^{-1} and *G*-mode has two main components TO and LO, situated at 1592 and 1568 cm^{-1}. The intensity of Raman scattering in unfilled PMMA stretched by the same manner as the composite film is quite low. The weak modes are situated at 260, 370, 490, 605, 1450 cm^{-1}. The Raman spectrum of stretched SWCNT/PMMA film shows the fingerprint modes of SWCNTs. The *G*-line maximum is slightly shifted to 1590 cm^{-1} due to the tension caused by the polymer stretch. The modes of PMMA are not distinguishable in the spectrum of composite.

To estimate the alignment of nanotubes in the stretched SWCNT/PMMA film, the Raman spectra were measured for the different relative orientations of the sample and

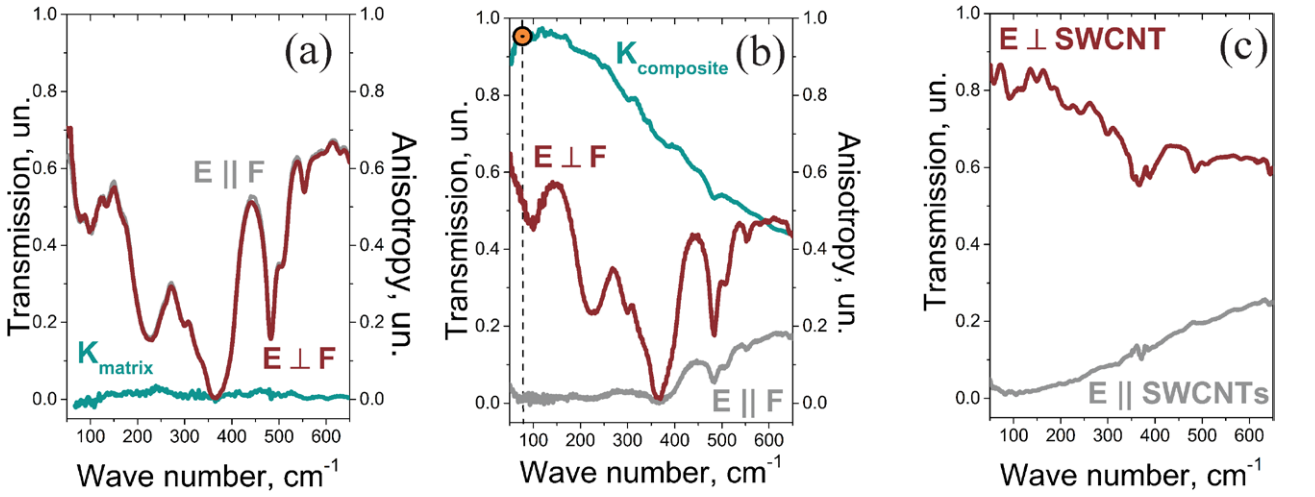

Figure 2. The transmission THz spectra for orthogonal and parallel orientation of light polarization (E) and stretching direction (F) and anisotropy coefficient K for (a) stretched PMMA matrix and (b) SWCNT/PMMA composite. (c) Contribution of nanotubes to transmission spectra of SWCNT/PMMA composite.

polarization of the incident light. Figures 1(b) and (c) presents the dependencies of Raman G-mode intensity on the sample orientation. Also the theoretical curves $I_{VV} \sim \cos^4\alpha$ and $I_{VH} \sim \cos^2\alpha \sin^2\alpha$ are shown for comparison. The presence of minima and maxima of the scattered light intensity is an unambiguous sign of nanotube alignment. The experimental data follow well the theoretical curves. However, there is an incomplete suppression of scattering in the minima of the dependencies for experimental data. The simplest explanation of this discrepancy is that there is an imperfect alignment of nanotubes, i.e. instead of one peculiar nanotube orientation there is a certain angular spread and distribution around the direction of the film stretch.

The ratio of Raman intensities at maxima and minima provides the estimation of distribution width of SWCNT orientations. For crossed and parallel polarisations of the incident and scattered light the ratio of intensities in minimum and maximum were 7 and 20, respectively. The Raman signal of the sample is the superposition of scattering from different SWCNTs, oriented in different directions. In VH configuration, for example, this is the following dependence: $I_{VH}(\alpha) = \int\varphi(\theta)\cos^2(\alpha-\theta)\sin^2(\alpha-\theta)\mathrm{d}\theta$, where α is the angle between the direction of incident light polarization and the SWCNT axis, and $\varphi(\theta)$ is the angular distribution of SWCNT axis orientations. Assuming the Gaussian shape of $\varphi(\theta)$, the experimental data let us to estimate the width of angular distribution. In case when the film was stretched 4 times, the halfwidth of the angular distribution of SWCNTs was 15°.

The further alignment of SWCNTs was complicated by obvious reasons. First, the stretched polymer/nanotube film after a certain elongation started to crack, and the folds are formed. Second, the alignment of SWCNTs could be hindered, if the nanotubes were crosslinked or bundled.

Due to the high anisotropy of obtained material in the visible spectral range the SWCNT/PMMA composite was investigated in THz region. To exclude the influence of stretched matrix, the transmission spectra polarized along and across the stretching direction for empty stretched PMMA matrix were recorded. The transmission spectra obtained for PMMA are shown in figure 2(a). The absorption bands of polymer are situated at 100, 225, 364, 482, 553 THz. Irrespectively of the orientation of PMMA film, its transmission spectrum is the same. To check additionally the stretching effect, the anisotropy factor K was calculated for the stretched matrix as a ratio of difference and sum of intensities of transmitted light, polarized orthogonal and parallel to the stretching direction: $K = (I_\perp - I_{||})/(I_\perp + I_{||})$. The coefficient K should be equal to 1 for an ideal polarizer and K is zero for an isotropic sample. One can see that for the stretched PMMA matrix the K value is near 0 in the whole investigated frequency range. Hence, it will be no influence of the stretched matrix to the signal registered from the SWCNT/PMMA composite.

Transmission of THz radiation through the stretched SWCNT/PMMA film for two different orientations of the sample to the incident light polarization is presented in figure 2(b). One can see that transmission of THz radiation through the composite depends on the relative orientation of SWCNTs in the sample and the light polarization direction. In case of orthogonal orientation of light polarization and stretching direction the transmission spectrum is quite similar to the spectrum of PMMA matrix with the set of absorption bands specific to the polymer. Otherwise, in case of co-directional light polarization and stretching direction the transmission coefficient is dramatically decreased. The experimental spectrum shows quite a high absorption value for this type of light in the range from 30 to 350 cm^{-1} and a slight increasing in the frequency range higher than 350 cm^{-1}.

The anisotropic coefficient K calculated for the investigated composite material is also presented in figure 2(b). As it can be seen the K value lies in the range from 0.4 to 0.97. The maximum K value about 0.97 was registered at 100 cm^{-1}. The high value of anisotropic transmission about 0.95 is observed in the frequency range from 50 to 250 cm^{-1}. Such a high anisotropy factor indicates that SWCNTs quite effectively absorbed and reflected radiation in case of their orientation in the direction of light polarization. In case of orthogonal orientation of

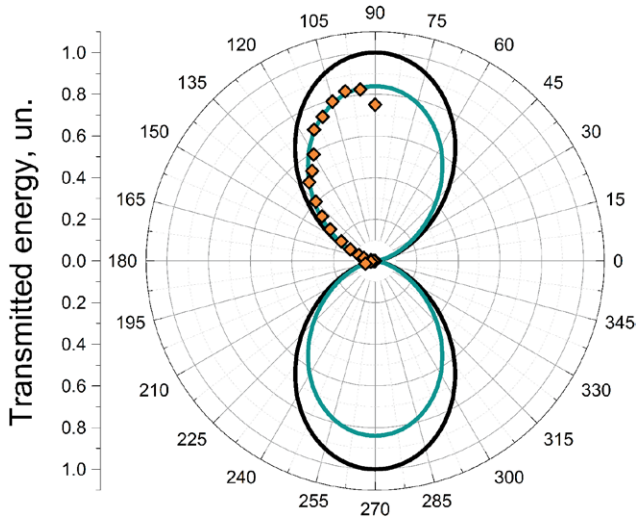

Figure 3. The experimental angular distribution of transmitted energy at wavelength 130 μm (diamonds) in comparison with the approximation made by $\sin^2(\theta)$ function for an ideal nanotube orientation (black curve) and an average misorientation of 12° (cyan curve).

SWCNT axis and light polarization, the influence of nanotube to the absorption process is negligible.

To confirm the effect of nanotubes to the registered absorption the optical densities of composite material and the matrix were calculated. From the difference of these two values the optical densities for SWCNT oriented along and across to the incident light polarization were obtained. The transmission spectra for SWCNTs oriented along and across to the light polarization were modeled from the obtained values of optical density (figure 2(c)). As it can be seen, SWCNTs demonstrate quite high polarized properties in the range from 50 to 250 cm^{-1}.

The angular distribution of energy transmission by SWCNT/PMMA film at wavelength of 130 μm (marked by dot in figure 2(b)) is shown in figure 3. The ratio of the highest and the lowest energy transmitted through the sample is equal to 52. The experimental results provided a possibility to estimate the distribution width of SWCNT orientations. Assuming the Gaussian distribution of SWCNT orientations, the intensity of transmitted radiation was calculated by $\sin^2(\theta)$ function for different widths of distribution. In figure 3 the results of modelling by $\sin^2(\theta)$ function for an ideal orientation of SWCNTs in the sample and for SWCNTs with an average misorientation $\omega \sim 12°$ are compared with the experimental results. One can see a good fitting of experimental results by the model with the halfwidth of the angular distribution of nanotubes $\omega \sim 12°$. The value obtained is smaller than the same parameter estimated from the Raman data.

As it can be seen, the difference between orientation parameters of SWNTs in the sample obtained by methods with wavelengths about 1 μm and 100 μm is not so significant. The decreasing the orientation order observed in the visible range can be attributed to the local deviations of nanotubes from the stretching direction. The increasing the wavelength up to THz region lead to the decreasing the contribution of these deviations to the signal registered and, the structure of composite in this region seems to have more ideal ordering of nanotubes in the sample than in the visible region. The average angle of deviations $\Delta\omega$ can be estimated as a difference between the squares of measured halfwidths of the angular distributions: $(\omega^2_{\mathrm{Vis}} - \omega^2_{\mathrm{THz}})^{1/2}$. The obtained value near ~9° is a characteristic parameter of nanotube bending in composite at the scale about ~1 μm.

To summarize, the anisotropic SWCNT/PMMA composites were produced by stretching the polymer films with dispersed filler at elevated temperature. The alignment of SWCNTs was estimated from Raman scattering and THz absorption polarized measurements. The Raman spectra measured in parallel and crossed orientations of polarization of the incident and scattered light showed a strong suppression of the SWCNT *G*-mode intensity at angles of $(2n + 1) \times \pi/2$ and $n \times \pi/2$, respectively. The largest absorption of 130 μm irradiation by the composite was observed when the polarization vector of THz light was parallel to the stretching direction. These results indicated a preferable orientation of SWCNTs in the direction of the applied stretching force. The approximation of angular dependencies of THz transmitted energy and Raman scattering has given a value of SWCNT misorientation of 12 and 15°, respectively. The difference of obtained values of misalignment in the sample for THz and Raman spectroscopy can be attributed to the different sensitivity of these methods to the deviation of nanotube from the straight ideal structure. Thus, SWCNT/PMMA composites demonstrated strong anisotropy of optical properties in the wide spectral range from visible to THz.

Acknowledgments

Authors would like to acknowledge the support of the Russian Foundation for Basic Research (RFBR), grants 15-02-08199 and 15-59-31817, for sample preparation and Raman measurements and grant 14-03-90028 for THz investigations. NRA thanks the RFBR for grant 14-32-50082. The NFEL was operated under the Russian Science Foundation support (project 14-50-00080).

References

[1] Ferguson B and Zhang X C 2002 *Nat. Mater.* **1** 26
[2] Tonouchi M 2007 *Nat. Photon.* **1** 97
[3] Federici J F, Schulkin B, Huang F, Gary D, Barat R, Oliveira F and Zimdars D 2005 *Semicond. Sci. Technol.* **20** S266
[4] Williams B S 2007 *Nat. Photon.* **1** 517
[5] Tanoto H *et al* 2012 *Nat. Photon.* **6** 121
[6] Rogalski A and Sizov F 2011 *Opto-Electron. Rev.* **19** 346
[7] Chen H-T, Padilla W J, Zide J M O, Gossard A C, Taylor A J and Averitt R D 2006 *Nature* **444** 597
[8] Hsieh C-F, Lai Y-C, Pan R-P and Pan C-L 2008 *Opt. Lett.* **33** 1174
[9] Wojdyla A and Gallot G 2011 *Opt. Express* **19** 14099
[10] Ren L *et al* 2009 *Nano Lett.* **9** 2610
[11] Ren L, Pint C L, Arikawa T, Takeya K, Kawayama I, Tonouchi M, Hauge R H and Kono J 2012 *Nano Lett.* **12** 787
[12] Kyoung J, Jang E Y, Lima M D, Park H-R, Robles R O, Lepró X, Kim Y H, Baughman R H and Kim D-S 2011 *Nano Lett.* **11** 4227

[13] Tian D-B, Zhang H-W, Lai W-E, Wen Q-Y, Song Y-Q and Wang Z-G 2010 *Chin. Phys. Lett.* **27** 104210
[14] Deng L Y, Teng J H, Zhang L, Wu Q Y, Liu H, Zhang X H and Chua S J 2012 *App. Phys. Lett.* **101** 011101
[15] Okotrub A V, Kubarev V V, Kanygin M A, Sedelnikova O V and Bulusheva L G 2011 *Phys. Status Solidi* b **248** 2568
[16] Kanygin M A, Selyutin A G, Okotrub A V and Bulusheva L G 2012 *Fullerenes Nanotubes Carbon Nanostruct.* **20** 523
[17] Bychanok D S, Shuba M V, Kuzhir P P, Maksimenko S A, Kubarev V V, Kanygin M A, Sedelnikova O V, Bulusheva L G and Okotrub A V 2013 *J. Appl. Phys.* **114** 114304
[18] Sedelnikova O V, Kanygin M A, Korovin E Y, Bulusheva L G, Suslyaev V I and Okotrub A V 2014 *Compos. Sci. Technol.* **102** 59
[19] Kocabas C, Hur S-H, Gaur A, Meitl M A, Shim M and Rogers J A 2005 *Small* **1** 1110
[20] Han S, Liu X and Zhou C 2005 *J. Am. Chem. Soc.* **127** 5294
[21] LeMieux M C, Sok S, Roberts M E, Opatkiewicz J P, Liu D, Barman S N, Patil N, Mitra S and Bao Z 2009 *ASC Nano* **3** 4089
[22] Zamora-Ledezma C, Blanc C, Maugey M, Zakri C, Poulin P and Anglaret E 2008 *Nano Lett.* **8** 4103
[23] Lu L and Chen W 2010 *ASC Nano* **4** 1042
[24] McLean R S, Huang X, Khripin C, Jagota A and Zheng M 2006 *Nano Lett.* **6** 55
[25] Li X, Zhang L, Wang X, Shimoyama I, Sun X, Seo W-S and Dai H 2007 *J. Am. Chem. Soc.* **129** 4890
[26] Engel M, Small J P, Steiner M, Freitag M, Green A A, Hersam M C and Avouris P 2008 *ASC Nano* **2** 2445
[27] Arutyunyan N R, Chernov A I, Kuznetsov K M and Obraztsova E D 2012 *J. Nanoelectron. Optoelectron.* **7** 1
[28] Arutyunyan N R, Chernov A I and Obraztsova E D 2010 *Phys. Status Solidi* b **247** 2814
[29] Ichida M, Mizuno S, Kataura H, Achiba Y and Nakamura A 2004 *Appl. Phys.* A **78** 1117
[30] Zamora-Ledezma C, Blanc C and Anglaret E 2009 *Phys. Rev.* B **80** 113407
[31] Zhou B, Lin Y, Veca L M, Fernando K A S, Harruff B A and Sun Y-P 2006 *J. Phys. Chem.* B **110** 3001
[32] Arutyunyan N R and Obraztsova E D 2013 *J. Nanoelectron. Optoelectron.* **8** 1
[33] Bychanok D S, Kanygin M A, Okotrub A V, Shuba M V, Paddubskaya A G, Pliushch A O, Kuzhir P P and Maksimenko S A 2011 *JEPT Lett.* **93** 607
[34] Obraztsova E D, Bonard J M and Kuznetsov V L 1998 *AIP Conf. Proc.: Electronic Properties of Novel Materials—Progress in Molecular Nanostructures: XII Int. Winter School* vol 442 p 132
[35] Obraztsova E D, Yurov V Y, Shevluga V M, Baranovsky R E, Nalimova V A, Kuznetsov V L and Zaikovskii V I 1999 *Nanostruct. Mater.* **11** 295